

Cyanine-Based Fluorescent Probe for Highly Selective Detection of Glutathione in Cell Cultures and Live Mouse Tissues

Jun Yin,^{†,‡,⊥} Younghee Kwon,^{§,||,⊥} Dabin Kim,[†] Dayoung Lee,[†] Gyoungmi Kim,[†] Ying Hu,[†] Ji-Hwan Ryu,^{*,§,||} and Juyoung Yoon^{*,†}

[†]Department of Chemistry and Nano Science, Global Top 5 Research Program, Ewha Womans University, Seoul 120-750, Korea

[‡]Key Laboratory of Pesticide and Chemical Biology of the Ministry of Education, College of Chemistry, Central China Normal University, Wuhan 430079, People's Republic of China

[§]Research Center for Human Natural Defense System and ^{||}BK 21 Plus Project for Medical Science, Yonsei University College of Medicine, Seoul 120-752, Korea

S Supporting Information

ABSTRACT: Glutathione (GSH) plays a crucial role in human pathologies. Near-infrared fluorescence-based sensors capable of detecting intracellular GSH *in vivo* would be useful tools to understand the mechanisms of diseases. In this work, two cyanine-based fluorescent probes, **1** and **2**, containing sulfonamide groups were prepared. Evaluation of the fluorescence changes displayed by probe **1**, which contains a 2,4-dinitrobenzenesulfonamide group, shows that it is cell-membrane-permeable and can selectively detect thiols such as GSH, cysteine (Cys), and homocysteine (Hcy) in living cells. The response of **1** to thiols can be reversed by treatment with *N*-methylmaleimide (NMM). Probe **2**, which possesses a 5-(dimethylamino)naphthalenesulfonamide group, displays high selectivity for GSH over Cys and Hcy, and its response can be reversed using NMM. The potential biological utility of **2** was shown by its use in fluorescence imaging of GSH in living cells. Furthermore, probe **2** can determine changes in the intracellular levels of GSH modulated by H₂O₂. The properties of **2** enable its use in monitoring GSH *in vivo* in a mouse model. The results showed that intravenous injection of **2** into a mouse generates a dramatic image in which strong fluorescence is emitted from various tissues, including the liver, kidney, lung, and spleen. Importantly, **2** can be utilized to monitor the depletion of GSH in mouse tissue cells promoted by excessive administration of the painkiller acetaminophen. The combined results coming from this effort suggest that the new probe will serve as an efficient tool for detecting cellular GSH in animals.



INTRODUCTION

Amino acids containing the thiol group are components of many peptides that play crucial roles in maintaining biological redox homeostasis in biological systems through an equilibrium between reduced free thiol and oxidized disulfide forms.¹ Importantly, numerous investigations have demonstrated that abnormal levels of these amino acids are closely associated with certain disease states, including liver damage, cancer, AIDS, osteoporosis, Alzheimer's disease, and heart, inflammatory bowel, and cardiovascular diseases.² Consequently, assessments of the levels of thiol-containing substances in biological systems may aid early diagnosis of some diseases. Over the past several decades, a considerable effort has been devoted to development of an effective strategy for the detection of thiols in living systems (biothiols). Among the various analytical methods that are available, molecular imaging based on fluorescence is considered to be the most sensitive approach owing to its sensitivity and simplicity. In recent years, numerous fluorescent probes have been developed that can distinguish biothiols from other amino acids by utilizing the fact that thiols undergo

unique nucleophilic addition and substitution reactions.³ However, the design of a highly selective detection system that discriminates between biothiols with similar structures and reactivities (e.g., cysteine (Cys), homocysteine (HCy), and glutathione (GSH)) is still a significant challenge.⁴

GSH, the most abundant intracellular nonprotein biothiol, serves many cellular functions, including maintenance of intracellular redox activity, xenobiotic metabolism, intracellular signal transduction, and gene regulation. This important biothiol protects cellular components from damage caused by free radicals and reactive oxygen species (ROS) and maintains exogenous antioxidants in their reduced forms.⁵ These properties suggest that highly selective methods to monitor and quantitate GSH under physiological conditions are of significant interest in clinical medicine⁶ and for investigations aimed at probing cellular functions.⁴

Received: December 12, 2013

Published: March 20, 2014

Thus far, several fluorescent probes based on organic dyes for highly selective detection of GSH have been designed. For example, in 2010 Yang and Chan described a promising GSH probe that is based on a bis-spiropyran structure.⁷ Recently, a resorufin-based probe was devised by Strongin to be used for the detection of GSH in human blood plasma in a highly selective manner.⁸ Yang has also developed a ratiometric, monochlorinated BODIPY-based fluorescence sensor, which is responsive to GSH and not Cys and Hcy and which can be employed for detection of GSH in living cells.⁹

Considering the fact that GSH is a major endogenous antioxidant present in the intracellular environment at concentration levels in the range of 0.5–10 mM, its *in vivo* detection using near-infrared (700–900 nm) fluorescent probes would have important advantages owing to the less biological damaging and deeper tissue penetration properties of light in this wavelength region.¹⁰ Although several near-infrared, cyanine-based fluorescent probes have been reported recently, they suffer from low thiol selectivity.¹¹ In the study described below, we developed two near-infrared, cyanine-based fluorescent probes (**1** and **2**, Scheme 1) each containing a

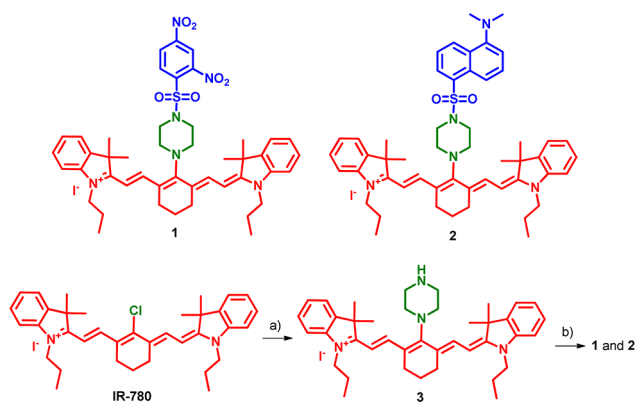
sulfonamide functional moiety. The results show that the fluorescent turn-on probe **1** can be used to detect GSH, Cys, and Hcy and that it is cell-membrane-permeable and applicable for thiol detection in living cells. More important is the observation that probe **2** displays a high selectivity for detection of GSH over Cys and Hcy and that it can be used to monitor GSH in cells. Furthermore, observations made in this effort show that injection of probe **2** into a mouse gives rise to a dramatic turn-on fluorescence image, with emission occurring from various tissues such as the liver, kidney, lung, and spleen.

RESULTS AND DISCUSSION

Near-infrared fluorescent probes, and especially those that are based on cyanine,¹² have gained increasing interest recently. In addition, the unique reactivity profile of thiols (e.g., promotion of sulfonamide cleavage) is a significant feature of the design of thiol-selective probes.³ In our design of the new thiol probes **1** and **2**, we selected cyanine as the near-infrared fluorophore and thiol-responsive sulfonamides as the reaction component. The sulfonamides, linked to the cyanine moiety through a piperazine bridge in **1** and **2**, undergo cleavage in the presence of thiols to form free piperazine **3** (Scheme 1) in concert with turn-on fluorescence.¹³ The routes used to prepare **1** and **2**, outlined in Scheme 1, begin with reaction of IR-780 with piperazine in DMF to produce intermediate **3**. Treatment of this substance with either 2,4-dinitrobenzene-1-sulfonyl chloride or dansyl chloride then efficiently leads to generation of the respective cyanine-based probes **1** and **2**.

Studies were carried out to explore the use of near-infrared fluorescent probe **1** to detect amino acids containing a thiol group. Analysis of UV/vis absorption spectroscopic changes shows that addition of a thiol (such as GSH or Cys or Hcy, 100 μM) to a solution of **1** (10 μM) in HEPES buffer (10 mM, pH 7.4) containing 10% DMSO leads to an increase in absorbance at 730 nm (Figure S1A, Supporting Information). Similarly, mixing **1** with a thiol leads to production of a fluorescence emission band with a maximum at 736 nm, while no obvious changes take place when other amino acids are added (Figure S1B). These observations suggest that **1** can be employed to detect thiols.

Scheme 1. Structures and Synthesis of Cyanine-Based Fluorescent Probes 1 and 2^a



^aReagents and conditions: (a) piperazine, DMF, 85 °C, 85%; (b) sulfonyl chloride, $\text{CH}_2\text{Cl}_2/\text{Et}_3\text{N}$, 75–82%.

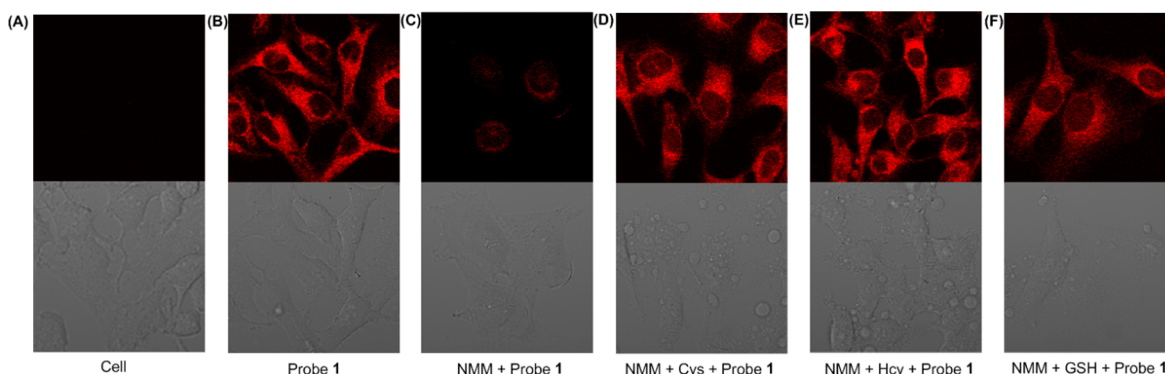


Figure 1. Confocal microscope images following addition of probe **1** to HeLa cells. Cell images were obtained using an excitation wavelength of 635 nm and a band-path (655–755 nm) emission filter. (A) Fluorescence image of HeLa cells. (B) Fluorescence image of HeLa cells incubated with probe **1** (10 μM) for 20 min. (C) Fluorescence image of HeLa cells pretreated with *N*-methylmaleimide (NMM; 1 mM) for 20 min and incubated with probe **1** (10 μM) for 20 min. (D) Fluorescence image of HeLa cells pretreated with NMM (1 mM) for 20 min and then added to cysteine (100 μM) and incubated with probe **1** (10 μM) for 20 min. (E) Fluorescence image of HeLa cells pretreated with NMM (1 mM) for 20 min and then added to homocysteine (100 μM) and incubated with probe **1** (10 μM) for 20 min. (F) Fluorescence image of HeLa cells pretreated with NMM (1 mM) for 20 min and then added to glutathione (100 μM) and incubated with probe **1** (10 μM) for 20 min.

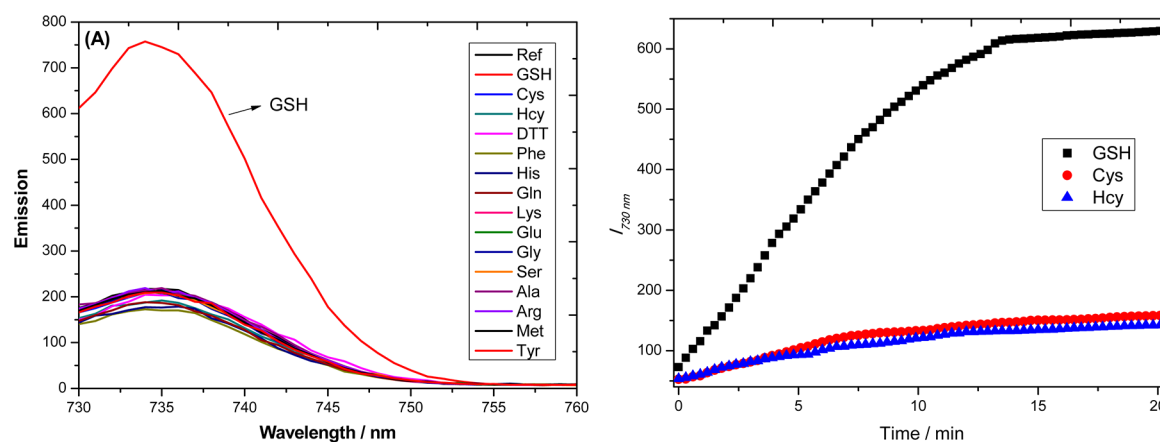


Figure 2. (A) Fluorescence response of probe 2 ($10\ \mu\text{M}$) to various amino acids ($100\ \mu\text{M}$). Each spectrum was recorded 20 min following addition of the amino acid. (B) Time-dependent fluorescence changes of probe 2 ($10\ \mu\text{M}$) upon addition of GSH, Cys, and Hcy ($100\ \mu\text{M}$) in HEPES ($10\ \text{mM}$, pH 7.4) containing 10% DMSO. $\lambda_{\text{ex}} = 730\ \text{nm}$, $\lambda_{\text{em}} = 736\ \text{nm}$, and the slit width was 10 nm.

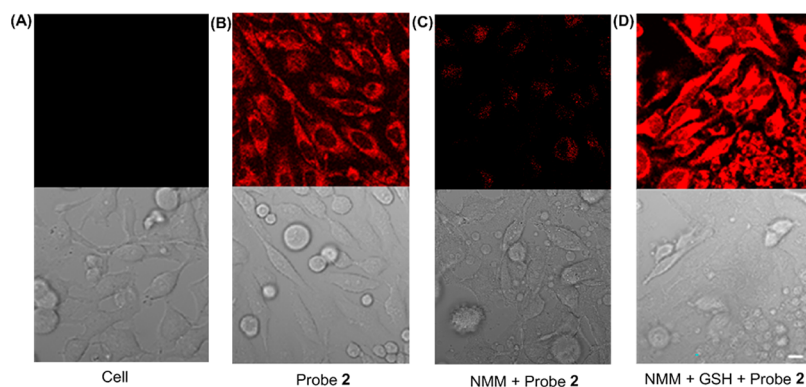


Figure 3. Confocal microscope images of probe 2 in HeLa cells. Cell images were obtained using an excitation wavelength of 635 nm and a band-pass (655–755 nm) emission filter. (A) Fluorescence image of HeLa cells. (B) Fluorescence image of HeLa cells incubated with probe 2 ($20\ \mu\text{M}$) for 20 min. (C) Fluorescence image of HeLa cells pretreated with NMM ($1\ \text{mM}$) for 20 min and incubated with probe 2 ($20\ \mu\text{M}$) for 20 min. (D) Fluorescence image of HeLa cells pretreated with NMM ($1\ \text{mM}$) for 20 min and then treated with GSH ($100\ \mu\text{M}$) for 20 min and incubated with probe 2 ($20\ \mu\text{M}$) for 20 min.

To determine the biological relevance of the new near-infrared fluorescent probe, studies were carried out to assess the use of **1** in fluorescence imaging of cellular thiols. For this purpose, HeLa cells were grown in RPMI 1640 (Roswell Park Memorial Institute) supplemented with 10% heat-inactivated fetal bovine serum, 100 U/mL penicillin, and 100 U/mL streptomycin and were maintained in an incubator at $37\ ^\circ\text{C}$ with a 5% CO_2 /air environment. As illustrated by viewing the confocal fluorescence microscope images displayed in Figure 1B and bright field images shown in Figure 1A, a significant red fluorescence image is produced in the cytoplasm when HeLa cells are incubated with probe **1** ($10\ \mu\text{M}$) at $37\ ^\circ\text{C}$ for 20 min (Figure 1B). The results suggest that **1** is capable of permeating into cells and reacting with resident thiols to produce discernible fluorescence images.

A series of control experiments were performed to gain support for this conclusion. The HeLa cells were pretreated with the thiol-blocking reagent *N*-methylmaleimide (NMM) for 20 min and then incubated with **1** ($10\ \mu\text{M}$) for 20 min. The resulting confocal microscope image (Figure 1C) does not display red fluorescence. Moreover, addition of Cys, Hcy, or GSH ($100\ \mu\text{M}$) to the NMM-pretreated HeLa cells gives rise to a significant increase in red emission (Figure 1D–F,

respectively). Thus, probe **1** can be employed to detect thiols in living cells.

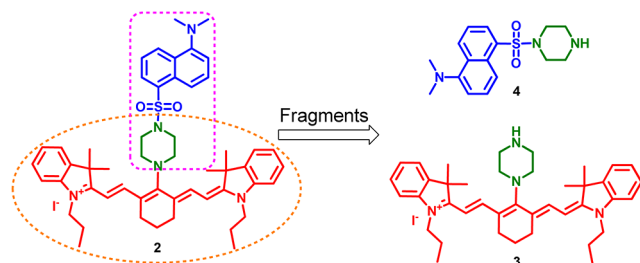
The results of studies, designed to assess the potential selectivity of the response of the probe toward various thiol-containing amino acids, show that **2** can be used to detect GSH selectively. Specifically, treatment of a solution of probe **2** ($10\ \mu\text{M}$) in HEPES buffer ($10\ \text{mM}$, pH 7.4) containing 10% DMSO with GSH ($100\ \mu\text{M}$) results in significant turn-on fluorescence at 736 nm (excitation at 730 nm) (Figure 2A) in a GSH-concentration-dependent manner (Figure S3, Supporting Information). The results of an experiment probing the time-dependent fluorescence response of probe **2** ($10\ \mu\text{M}$) to GSH ($100\ \mu\text{M}$) at $37\ ^\circ\text{C}$ in HEPES buffer solution ($10\ \text{mM}$, pH 7.4) containing 10% DMSO show that the intensity of the 736 nm emission band increases with time, reaching a maximum in less than 15 min (Figure S4, Supporting Information). Compared to GSH, the other thiol-based amino acids, Cys and Hcy, do not promote as rapid a fluorescence response of probe **2** (Figure 2B). Subsequent investigation in human serum is performed. According to the fluorescence spectra (Figure S5, Supporting Information), we find that the fluorescence intensity will increase along with the addition of human serum owing to the existence of GSH in serum.

To gain support for the proposal that treatment of probes 1 and 2 with thiols promotes fluorescence through chemical reactions that liberate free piperazine 3, the processes were probed using mass spectrometry. For this purpose, a soft ionization method, based on matrix-assisted laser ionization (MALDI), was employed to follow reactions of the probes with thiols. Formation of the thiolysis product 3 in reactions of probe 1 with GSH, Cys, and Hcy was identified by using MALDI-TOF mass spectrometry (in Figure S6, Supporting Information). In addition, this method was used to show that GSH cleaves the sulfonamide group of probe 2 to form 3 under the same conditions (in Figure S7 and Scheme S1, Supporting Information).

To demonstrate its cellular GSH fluorescence imaging capability, probe 2 was incubated with living HeLa cells at 37 °C for 20 min. Red fluorescence emission was observed inside the cells by using a confocal fluorescence microscope (Figure 3A,B), demonstrating that 2 is readily internalized into living cells. NMM was employed as a thiol-blocking reagent in a control experiment. A markedly lower fluorescence intensity increase takes place when the HeLa cells are pretreated with NMM for 20 min and then incubated with probe 2 (10 μ M) for 20 min (Figure 3C). Moreover, addition of a high concentration of GSH (100 μ M) to this solution and incubation for another 20 min leads to production of a strong red fluorescence image (Figure 3D) in the same field of view. These findings demonstrate that probe 2 has excellent cell permeability and that it can be utilized to monitor GSH in living cells. Even though the selectivity of probe 2 for GSH in solution has been demonstrated, its ability to selectively detect this thiol in cells requires investigation. Experiments in which the thiol-blocking reagent NMM is employed were ideal for this purpose. Accordingly, HeLa cells were pretreated with NMM for 20 min and then incubated with probe 2 (10 μ M) for 20 min. As expected, the confocal microscope image of the cells treated in this manner does not display red fluorescence. Moreover, addition of Cys or Hcy (100 μ M) to the NMM-pretreated HeLa cells give rise to only small changes in the fluorescence intensity. In contrast, addition of GSH (100 μ M) does promote a significant increase in red emission (Figures S8, Supporting Information).

The results of the experiments described above clearly confirm that, in comparison to probe 1, probe 2 possesses a high selectivity toward GSH in both solution and living cells. Additional experiments were designed to gain a better understanding of the source of this selectivity. As shown in Scheme 2, probe 2 is comprised of two fragments represented by model compounds 3 and 4, which contain a common piperazine moiety. Compound 4 was prepared using the previously described method¹⁴ so that its response to GSH

Scheme 2. Fragments 3 and 4 of Probe 2



could be determined. The results show that GSH does not perturb the UV–vis absorption and fluorescence spectra of 4 (Figure S9, Supporting Information). In addition, we demonstrated that GSH also does not promote changes in the UV–vis and fluorescence spectra of 3 (Figure S10, Supporting Information). These observations suggest that 3 and 4, which represent the independent components of probe 2, do not respond to GSH.

Results arising from earlier studies suggest that the conformation of the piperazine ring is a very important factor in governing sensing selectivities.^{14,15} The piperazine rings in 1–4, like that of cyclohexane, can exist in both chair and boat conformations. It is possible that these conformational preferences play a role in governing the selectivities in responses to thiols.¹⁶ Consequently, a more detailed analysis of the structure and conformation of probe 2 was carried out in an attempt to gain insight into its selective response to GSH. Accordingly, density functional theory (DFT) calculations were used to optimize the structures of 1–4 at the B3LYP/6-31G* level using a suite of Gaussian 09 programs.

The results of the calculations show that the piperazine ring in 4 exists in a twist-boat conformation while the ring in 3 displays a classic chair conformation (Figure 4B,C). While the

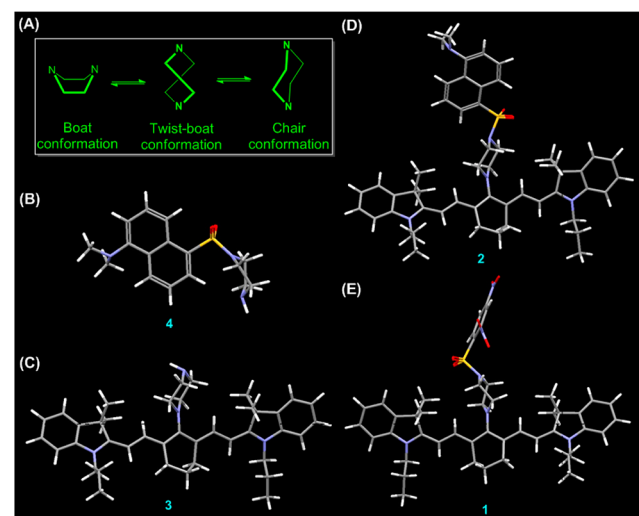


Figure 4. (A) Boat, twist-boat, and chair conformations of the piperazine ring. Optimized, low-energy conformations of the piperazine rings in 1–4 using DFT (B3LYP/6-31G*) calculations: (B) compound 4, (C) compound 3, (D) probe 2, (E) probe 1.

piperazine rings in probe 2 and compound 3 (Figure 4D) also possess chair conformations, the ring in probe 1 exists in a twist-boat conformation (Figure 4E). Even though the piperazine rings of 2 and 3 have similar chair conformations, the N–H hydrogen in 3 is axially oriented while the dansyl sulfonamide moiety in 2 is equatorially disposed. These findings suggest that the preference for piperazine ring chair conformations and the equatorial spatial disposition of the sulfonamide groups in probe 2 might be a significant feature determining the selective response to GSH.

From another perspective, the sulfur–nitrogen bond (S–N) lengths in these substances, which are likely related to bond strengths, differ in an interesting manner. For example, the respective S–N bond lengths in 1 and 4 are 1.667 and 1.660 Å. In contrast, probe 2 has a S–N bond length of 1.727 Å, which suggests that the S–N bond in this substance is weaker than the

analogous bond in probe 1. Finally, the obvious structural difference between GSH and the other thiols could be another source of the differences seen in reactivities with the sulfonamide moiety in the probes. GSH contains two amide units, and it has a longer flexible backbone in comparison to Cys and Hcy, which provides a possibility to form some intermolecular interaction with the probe such as hydrogen bonds. For that, we optimize the binding structure of probe 2 with GSH (Figure S12, Supporting Information), in which amide units of GSH can form the relevant hydrogen bonds (such as C–H...N and C–H...O) with the piperazine ring unit of probe 2. Besides, there is a possible electrostatic interaction between the indolium cation of probe 2 and the carbonate anion of GSH from the binding structure. Therefore, these intermolecular interactions will result in a closer distance of two reactive sites (SH group and sulfonamide group), possibly a reason for the higher reactivity of GSH. Moreover, it also affords an idea to design probes with high selectivity from the guest molecule's viewpoint.

Observations made in additional studies show that probe 2 can also be employed to detect the oxidant-governed redox status of GSH in living cells. As seen by viewing the confocal fluorescence microscope images displayed in Figure 5, addition

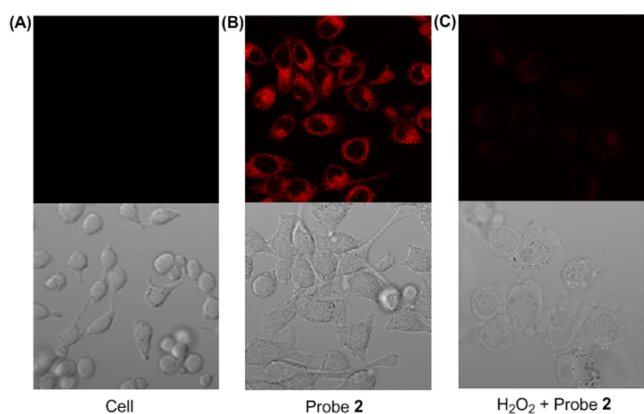


Figure 5. Confocal microscope images of probe 2 in HeLa cells. Cell images were obtained using an excitation wavelength of 635 nm and a band-path (655–755 nm) emission filter. (A) Fluorescence image of HeLa cells. (B) Fluorescence image of HeLa cells incubated with probe 2 (20 μM) for 20 min. (C) Fluorescence image of HeLa cells pretreated with H_2O_2 (100 μM) for 20 min and incubated with probe 2 (20 μM) for 20 min.

of H_2O_2 (100 μM) to a solution containing HeLa cells and probe 2 (Figure 5B) promotes a marked decrease in the fluorescence intensity (Figure 5C). This finding is likely the consequence of the alteration of the intracellular GSH concentration through oxidation promoted by H_2O_2 . An experiment was performed to confirm this proposal. As described above, compound 3 is the likely product of reaction between probe 2 and GSH. When 3 is added to H_2O_2 -treated living HeLa cells, an evident red fluorescence can be observed (Figure S11, Supporting Information). When the cells are pretreated with NMM for 20 min and then incubated with compound 3 (10 μM) for 20 min, no obvious fluorescence can be observed. These results suggest that the fluorescence caused by treating cells with probe 2 and GSH does not arise from the reaction of 3 with intracellular H_2O_2 . Therefore, the results of this experiment show that probe 2 can be used as a tool to monitor the level of intracellular GSH. Additionally, lip-

opolysaccharides (LPSs) are large molecules consisting of lipid and polysaccharide units that act as endotoxins to elicit strong immune responses in animals. Hence, the results of investigations of the effects of LPS on cells provide a greater understanding of the immune systems.¹⁷ As images displayed in Figure 6 show, a dramatic fluorescence decrease occurs when a

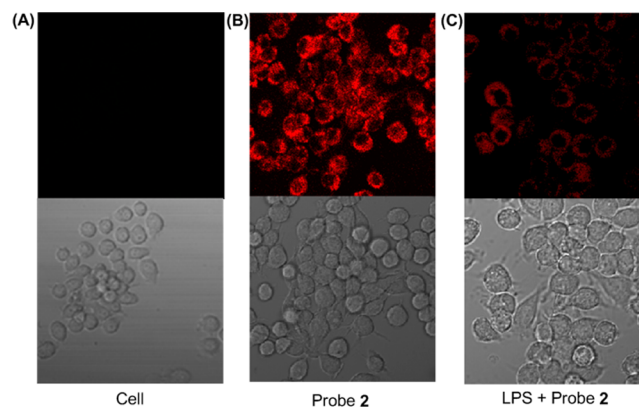


Figure 6. Confocal microscope images of probe 2 in RAW 264.7 cells. Cell images were obtained using an excitation wavelength of 635 nm and a band-path (655–755 nm) emission filter. (A) Fluorescence image of RAW 264.7 cells. (B) Fluorescence image of RAW 264.7 cells incubated with probe 2 (20 μM) for 20 min. (C) Fluorescence image of RAW 264.7 cells pretreated with lipopolysaccharide (LPS; 1 $\mu\text{g}/\text{mL}$) for 20 min, interferon γ (IFN- γ ; 50 ng/mL) for 16 h, and phorbol 12-myristate 13-acetate (PMA; 2.5 $\mu\text{g}/\text{mL}$) for 30 min and incubated with probe 2 (20 μM) for 20 min.

solution of HeLa cells is treated with LPS prior to the addition of 2. This observation indicates that LPS as an inhibitor could induce the fluorescence response in living cells.

To gain better insight into the molecular orbitals, the structures and frontier molecular orbital profiles were optimized by the DFT calculations at the B3LYP/6-31G* level in a suite of Gaussian 09 programs. Figure S11 (Supporting Information) presents the frontier molecular orbital profiles, which show that the different functional groups on the piperazine ring had heavy effects, especially for probes 1 and 2 (Figure S13, Supporting Information), and the calculated HOMO–LUMO energy gaps (2.14 and 2.13 eV for probes 1 and 2, respectively) were approximately the same as that of the thiolysis product 3 (2.22 eV). The lower band gaps further imply that two probes could be used as the near-infrared fluorescent dyes for imaging in vivo.

The results obtained from cell studies suggest that probe 2 has the potential of being used to detect GSH in vivo. To evaluate this proposal, mice were intravenously injected with buffer solutions containing 2 (50 μM) and then after 20 min observed using fluorescence imaging with an in vivo imaging system (IVIS). Strong fluorescence was observed to emanate from inside the mouse body (Figure 7). Moreover, when the mice were pretreated with NMM (20 mM for 20 min) and then injected with 2, a dramatically lower intensity fluorescence image was observed (Figure 7). Mice not treated with probe 2 or treated with only NMM do not show specific fluorescence under similar imaging conditions. To explore the location of probe 2 based in vivo detection of GSH, four mice, which were previously treated with 2, were dissected to isolate various tissues. In accordance with the whole-body mouse images, strong fluorescence was observed in various tissues, including

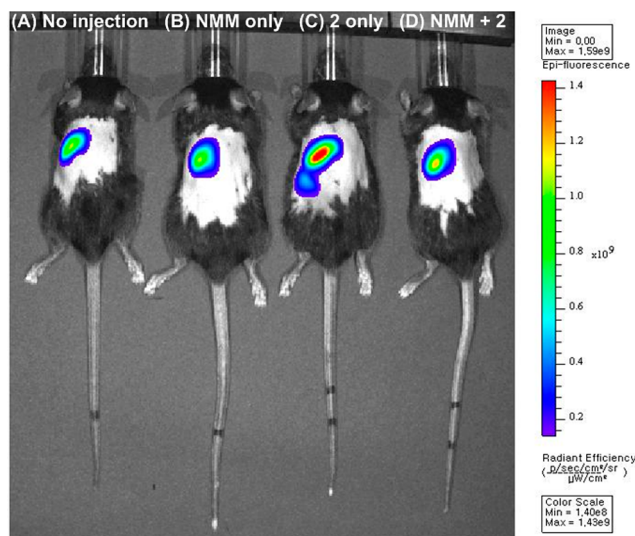


Figure 7. In vivo images of a mouse injected with probe 2 ($50 \mu\text{M}$) or NMM (20 mM) via intravenous injection for 20 min. Fluorescence images of (A) the mouse not injected with probe 2 (no injection), (B) the mouse injected with NMM (NMM only), (C) the mouse injected with probe 2 (2 only), and (D) the mouse injected with probe 2 after being preinjected with NMM (NMM + 2).

the liver, kidney, lung, and spleen. Importantly, fluorescence in these tissues was attenuated when the mice were pretreated with NMM (Figure S14, Supporting Information).

We have accumulated evidence that shows that probe 2 does not initially react with SH-group-containing serum proteins and biomolecules in the blood to form adducts that are then delivered into different organs. For this purpose, liver, lung, kidney, and spleen tissues were treated with probe 2 ($20 \mu\text{M}$ for 20 min). Strong fluorescence signals, having intensities that are similar to those coming from probe 2 treated mice, were observed to arise from the treated tissues (Figure S15, Supporting Information). Moreover, when mice were pretreated with NMM (20 mM for 20 min) via intravenous injection and then directly administered probe 2, lower intensity fluorescence images were observed (Figure S15). These results indicate that probe 2 can be employed to detect different concentrations of thiols in specific tissues directly.

The use of excessive amounts of certain drugs often causes damage to some tissues. For example, acetaminophen (APAP) is a safe painkiller when utilized at therapeutic levels. However, an overdose of this drug can cause severe liver damage¹⁸ and a depletion of GSH in liver and kidney cells.¹⁹ Thus, we examined the capability of probe 2 to detect acetaminophen-promoted tissue cell damage associated with a decrease in the level of GSH. Probe 2 based analysis of whole bodies and various tissues (Figure 8) shows that pretreatment of mice by intravenous injection with acetaminophen promotes a dramatic decrease in the fluorescence intensities in liver, kidney, lung, and spleen tissues (Figure 9). These observations clearly demonstrate that 2 is an effective probe for cellular GSH at the organism level.

CONCLUSION

In summary, the study described above has resulted in the development of two near-infrared fluorescent probes that contain a cyanine fluorophore linked to sulfonamide functional groups that undergo reactions with thiols. One of the probes,

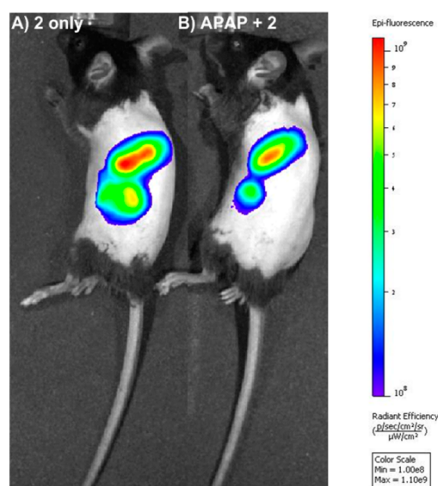


Figure 8. In vivo images of a mouse injected with probe 2 ($50 \mu\text{M}$) or acetaminophen (APAP; 300 mg/kg in 200 μL of HEPES buffer solution) via intravenous injection for 20 min. Fluorescence images of (A) the mouse injected with probe 2 (2 only) and (B) the mouse injected with probe 2 after being preinjected with APAP (APAP + 2).

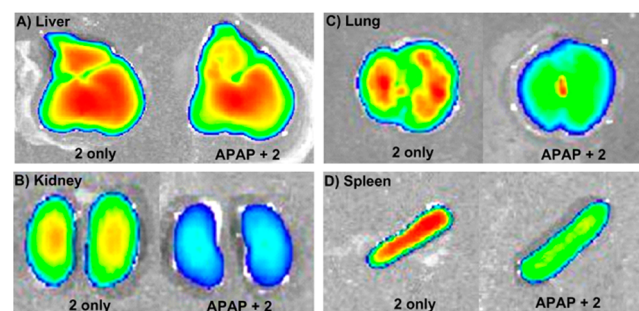


Figure 9. In vivo images of tissues from a mouse intravenously injected with probe 2 ($50 \mu\text{M}$) or acetaminophen (APAP; 300 mg/kg in 200 μL of HEPES buffer solution). Fluorescence images of the (A) liver, (B) kidney, (C) lung, and (D) spleen dissected from a mouse injected with probe 2 (2 only) and a mouse injected with probe 2 after being preinjected with APAP (APAP + 2).

which contains a 2,4-dinitrobenzenesulfonamide group, can be used to detect the thiol-based amino acids GSH, Cys, and Hcy in living cells. The other, possessing a 5-(dimethylamino)-naphthalenesulfonamide unit, displays unique selectivity toward GSH over Cys and Hcy. In addition, the latter probe is cell-membrane-permeable, and as a result, it can be employed to detect GSH in living cells. Finally, the latter near-infrared fluorescent probe can be used to monitor GSH levels in mouse tissues such as the liver, kidney, lung, and spleen. The results of this effort strongly suggest that the GSH-selective probe developed in this investigation can serve as an effective tool for studies probing cellular functions that are related to GSH.

EXPERIMENTAL SECTION

General Methods. All reactions and assembly processes were carried out under an argon atmosphere by using standard Schlenk techniques, unless otherwise stated. All starting materials and reagents, such as anhydrous *N,N*-dimethylformamide (DMF), dichloromethane (DCM), triethylamine (Et_3N), and human serum, were obtained commercially. ^1H and ^{13}C NMR spectra used CDCl_3 solutions and a Bruker AM-300 spectrometer with tetramethylsilane (TMS) as the internal standard. Mass spectra were measured in the ESI or MALDI mode. UV-vis spectra were obtained using a Scinco 3000

spectrophotometer (1 cm quartz cell) at 25 °C. Fluorescence spectra were recorded on an RF-5301/PC (Shimada) fluorescence spectrophotometer (1 cm quartz cell) at 25 °C. Deionized water was used to prepare all aqueous solutions.

Synthesis of 3. To a solution of IR-780 iodine (134 mg, 0.2 mmol) in anhydrous DMF (10 mL) under an argon atmosphere was added piperazine (69 mg, 0.8 mmol). After being stirred for 4 h at 85 °C, the mixture was cooled to room temperature. Removal of solvent under reduced pressure and purification by silica gel column chromatography with dichloromethane/methanol (40:1) as the eluent generated **3** as a blue solid: yield 136 mg, 85%; ¹H NMR (300 MHz, CDCl₃) δ 7.66 (d, *J* = 15.0 Hz, 2H), 7.26–7.32 (m, 4H), 7.09 (t, *J* = 6.0 Hz, 2H), 6.97 (d, *J* = 6.0 Hz, 2H), 5.80 (d, *J* = 15.0 Hz, 2H), 3.88 (m, 8H), 3.26 (t, *J* = 6.0 Hz, 4H), 2.44 (t, *J* = 6.0 Hz, 4H), 1.84 (m, 6H), 1.68 (s, 12H), 1.02 (t, *J* = 6.0 Hz, 6H); ¹³C NMR (75 MHz, CDCl₃) δ 173.3, 169.1, 142.8, 141.0, 140.3, 128.3, 123.7, 123.5, 122.2, 109.4, 85.9, 55.3, 48.2, 47.2, 45.2, 29.2, 25.0, 21.8, 20.3, 11.8; ESI MS *m/z* 589.6 [M – I]⁺, calcd exact mass 716.3.

Synthesis of 1. To a solution of **3** (143 mg, 0.2 mmol) in anhydrous dichloromethane (10 mL) under an argon atmosphere was added Et₃N (30 mg, 0.3 mmol). After the resulting solution was stirred for 5 min, a solution of 2,4-dinitrobenzene-1-sulfonyl chloride (53 mg, 0.2 mmol) in dichloromethane (5 mL) was added dropwise at 0 °C. Further stirring for 4 h at room temperature was followed by solvent removal under reduced pressure and purification by silica gel column chromatography with dichloromethane/methanol (30:1) as the eluent to produce **1** as a blue solid: yield 142 mg, 75%; ¹H NMR (300 MHz, CDCl₃) δ 8.77 (m, 2H), 8.52 (s, 1H), 7.80 (d, *J* = 15.0 Hz, 2H), 7.35 (m, 4H), 7.21 (m, 2H), 7.06 (d, *J* = 9.0 Hz, 2H), 5.95 (d, *J* = 15.0 Hz, 2H), 3.96 (t, *J* = 6.0 Hz, 4H), 3.76 (d, *J* = 6.0 Hz, 4H), 3.69 (d, *J* = 6.0 Hz, 4H), 2.49 (t, *J* = 6.0 Hz, 4H), 1.86 (m, 6H), 1.66 (s, 12H), 1.05 (t, *J* = 6.0 Hz, 6H); ¹³C NMR (75 MHz, CDCl₃) δ 170.4, 169.9, 149.8, 147.9, 142.5, 141.9, 140.5, 136.8, 134.9, 128.6, 127.8, 126.3, 124.5, 122.2, 119.4, 110.0, 98.2, 54.0, 48.6, 47.8, 45.6, 28.9, 25.3, 21.5, 20.6, 11.7; MALDI-TOF MS *m/z* 820.5 [M – I]⁺, calcd exact mass 946.3.

Synthesis of 2. To a solution of **3** (143 mg, 0.2 mmol) in anhydrous dichloromethane (10 mL) under an argon atmosphere was added Et₃N (30 mg, 0.3 mmol). After the resulting solution was stirred for 5 min, a solution of dansyl chloride (54 mg, 0.2 mmol) in dichloromethane (5 mL) was added dropwise at 0 °C. Further stirring for 4 h at room temperature was followed by removal of solvent under reduced pressure and purification by silica gel column chromatography with dichloromethane/methanol (30:1) as the eluent to yield **2** as a blue solid: yield 156 mg, 82%; ¹H NMR (300 MHz, CDCl₃) δ 8.76 (d, *J* = 9.0 Hz, 1H), 8.60 (d, *J* = 9.0 Hz, 1H), 8.32 (d, *J* = 9.0 Hz, 1H), 7.59–7.70 (m, 5H), 7.36 (m, 2H), 7.18–7.28 (m, 4H), 7.08 (d, *J* = 9.0 Hz, 2H), 5.95 (d, *J* = 15.0 Hz, 2H), 3.99 (t, *J* = 6.0 Hz, 4H), 3.55 (d, *J* = 6.0 Hz, 4H), 3.41 (d, *J* = 6.0 Hz, 4H), 2.96 (s, 6H), 2.47 (t, *J* = 6.0 Hz, 4H), 1.83 (m, 6H), 1.29 (s, 12H), 1.02 (t, *J* = 6.0 Hz, 6H); ¹³C NMR (75 MHz, CDCl₃) δ 170.4, 168.9, 152.0, 142.5, 141.7, 140.5, 132.0, 130.9, 130.1, 128.7, 128.6, 127.2, 124.4, 123.6, 122.0, 110.3, 98.8, 53.3, 48.3, 47.6, 45.8, 45.6, 28.2, 25.4, 21.5, 20.6, 11.7; MALDI-TOF MS *m/z* 822.7 [M – I]⁺, calcd exact mass 949.4.

Cell Culture. HeLa cells (human epithelial adenocarcinoma) and RAW 264.7 cells (mouse leukemic monocyte macrophage) were purchased from the Korean Cell Line Bank (Seoul, Korea). The cells were grown in RPMI 1640 supplemented with 10% heat-inactivated fetal bovine serum, penicillin (100 U/mL), and streptomycin (100 U/mL). All cells were maintained in an incubator at 37 °C with a 5% CO₂/air environment.

Confocal Microscope Imaging. Cells were seeded in 35 mm glass-bottomed dishes at a density of 3 × 10⁵ cells per dish in RPMI 1640 medium. After 24 h, probes (20 μM) were added to the cells, and the cells were incubated for 20 min at 37 °C. After being washed with Dulbecco's phosphate-buffered saline (DPBS) twice to remove the residual probe, the cells were imaged by using a confocal laser scanning microscope (Fluoview 1200, Olympus, Japan). The cells were excited by a 635 nm laser diode and detected at BA = 655–755 nm.

For control experiments, one group was treated with NMM (1 mM) for 20 min. Another group was pretreated with NMM (1 mM)

for 20 min and then incubated with probes (20 μM) for 20 min. The others were treated with additional GSH or Cys or Hcy (100 μM) at the same field of view.

For the H₂O₂ experiment, the cells were treated with H₂O₂ (100 μM) for 30 min at 37 °C and then incubated with probe **2** (20 μM) for 20 min at 37 °C.

RAW 264.7 cells were pretreated with LPS (1 μg/mL) for 20 min, interferon γ (IFN-γ; 50 ng/mL) for 16 h, and PMA (phorbol 12-myristate 13-acetate; 2.5 μg/mL) for 30 min.

HeLa cells were incubated with probes (10 μM) for 20 min at 37 °C, washed twice with DPBS, and imaged by using a confocal laser scanning microscope. Cell images were acquired with an excitation 635 nm laser diode and emission filter with BA = 655–755 nm. Next the HeLa cells were pretreated with NMM (1 mM) for 20 min and then with GSH or Cys or Hcy (100 μM) for 20 min and incubated with probes (20 μM) for 20 min.

Animals. We obtained 7–8 week old female C57BL/6 mice from the Jackson Laboratory (Bar Harbor, ME). All animal experiments were performed in a facility approved by the Association for Assessment and Accreditation of Laboratory Animal Care using protocols approved by the Department of Laboratory Animal Resources, Yonsei Biomedical Research Institute, Yonsei University College of Medicine.

In Vivo Imaging. C57BL/6 mice (female, 7–8 weeks old, Jackson Laboratory) were intravenously injected with NMM (20 mM, in 200 μL of HEPES buffer solution (10 mM, pH 7.4)). After 20 min, the mice were iv injected with probe **2** (50 μM, 200 μL). The back fur was removed using a depilatory cream, and the mouse imaging was performed with an IVIS Spectrum (Caliper Life Sciences, Hopkinton, MA) in epifluorescence mode equipped with 675 and 720 nm filters for excitation and emission, respectively, starting 20 min after probe **2** injection. Quantitative measurements of the fluorescence signal were made with Living Image Software 4.3.1 (Caliper Life Sciences).

The mice were injected with APAP (300 mg/kg in 200 μL of HEPES buffer solution). After 30 min, the mice were iv injected with probe **2** (50 μM, 200 μL).

For organ imaging, the mice were euthanized and the organs were dissected after in vivo imaging experiments. For ex vivo organ imaging, the liver, kidney, lung, and spleen were obtained from a mouse not injected with probe **2**, and the fluorescence image of those tissues directly treated with probe **2** (20 μM for 20 min) was obtained. The isolated liver, kidney, lung, and spleen were imaged with the IVIS Spectrum.

■ ASSOCIATED CONTENT

● Supporting Information

UV/vis absorption and fluorescence spectra of probes **1** and **2**, mass spectra after treatment of probes **1** and **2** with thiols, fluorescence images of mouse tissues, frontier molecular orbital profiles, and ¹H NMR, ¹³C NMR, and MS spectra of **1**, **2**, and **3**. This material is available free of charge via the Internet at <http://pubs.acs.org>.

■ AUTHOR INFORMATION

Corresponding Authors

yjh@yuhs.ac

jyoon@ewha.ac.kr

Author Contributions

¹J.Y. and Y.K. contributed equally to this work.

Notes

The authors declare no competing financial interest.

■ ACKNOWLEDGMENTS

This research was supported by a grant from the National Creative Research Initiative programs of the National Research Foundation of Korea (NRF) funded by the Korean government

(Ministry of Science, ICT and Future Planning, MSIP) (2012R1A3A2048814) and by the Basic Science Research Program through the NRF funded by the Ministry of Education (Grant 2013R1A1A200), and by the Bio & Medical Technology Development Program of the NRF funded by MSIP (NRF-2013M3A9D5072551). We thank Dr. Zhiqian Guo for his suggestion.

REFERENCES

- (1) Wood, Z. A.; Schroder, E.; Robin Harris, J.; Poole, L. B. *Trends Biochem. Sci.* **2003**, *28*, 32.
- (2) For selected literature, see: (a) Herzenberg, L. A.; De Rosa, S. C.; Dubs, J. G.; Roederer, M.; Anderson, M. T.; Ela, S. W.; Deresinski, S. C.; Herzenberg, L. A. *Proc. Natl. Acad. Sci. U.S.A.* **1997**, *94*, 1967. (b) Jacobsen, D. W. *Clin. Chem.* **1998**, *44*, 1833. (c) Shahrokhian, S. *Anal. Chem.* **2001**, *73*, 5972. (d) Townsend, D. M.; Tew, K. D.; Tapiero, H. *Biomed. Pharmacother.* **2003**, *57*, 145. (e) Tsien, R. Y. *Nat. Rev. Mol. Cell Biol.* **2003**, *4*, SS16–SS21. (f) Meade, T. J.; Aime, S. *Acc. Chem. Res.* **2009**, *42*, 821. (g) Hilderbrand, S. A.; Weissleder, R. *Curr. Opin. Chem. Biol.* **2010**, *14*, 71. (h) Ueno, T.; Nagano, T. *Nat. Methods* **2011**, *8*, 642. (i) Pittet, M. J.; Weissleder, R. *Cell* **2011**, *147*, 983. (j) James, M. L.; Gambhir, S. S. *Physiol. Rev.* **2012**, *92*, 897. (k) Chang, P. V.; Bertozzi, C. R. *Chem. Commun.* **2012**, *48*, 8864.
- (3) For selected reviews, see: (a) Yin, L.-L.; Chen, Z.-Z.; Tong, L.-L.; Xu, K.-H.; Tang, B. *Chin. J. Anal. Chem.* **2009**, *37*, 1073. (b) Chen, X.; Zhou, Y.; Peng, X.; Yoon, J. *Chem. Soc. Rev.* **2010**, *39*, 2120. (c) Zhou, Y.; Yoon, J. *Chem. Soc. Rev.* **2012**, *41*, 52. (d) Jung, H. S.; Chen, X.; Kim, J. S.; Yoon, J. *Chem. Soc. Rev.* **2013**, *42*, 6019. (e) Yin, C.; Huo, F.; Zhang, J.; Martínez-Mañez, R.; Yang, Y.; Lv, H.; Li, S. *Chem. Soc. Rev.* **2013**, *42*, 6032.
- (4) For selected literature, see: (a) Zhang, M.; Yu, M.; Li, F.; Zhu, M.; Li, M.; Gao, Y.; Li, L.; Liu, Z.; Zhang, J.; Zhang, D.; Yi, T.; Huang, C. *J. Am. Chem. Soc.* **2007**, *129*, 10322. (b) Tang, B.; Xing, Y.; Li, P.; Zhang, N.; Yu, F.; Yang, G. *J. Am. Chem. Soc.* **2007**, *129*, 11666. (c) Guy, J.; Caron, K.; Dufresne, S.; Michnick, S. W.; Skene, W. G.; Keillor, J. W. *J. Am. Chem. Soc.* **2007**, *129*, 11969. (d) Sreejith, S.; Divya, K. P.; Ajayaghosh, A. *Angew. Chem., Int. Ed.* **2008**, *47*, 7883. (e) Lee, J. H.; Lim, C. S.; Tian, Y. S.; Han, J. H.; Cho, B. R. *J. Am. Chem. Soc.* **2010**, *132*, 1216. (f) Yang, X.; Guo, Y.; Strongin, R. M. *Angew. Chem., Int. Ed.* **2011**, *50*, 10690. (g) Lee, M. H.; Han, J. H.; Kwon, P.-S.; Bhuniya, S.; Kim, J. Y.; Sessler, J. L.; Kang, C.; Kim, J. S. *J. Am. Chem. Soc.* **2012**, *134*, 1316. (h) Shao, J.; Sun, H.; Guo, H.; Ji, S.; Zhao, J.; Wu, W.; Yuan, X.; Zhang, C.; James, T. D. *Chem. Sci.* **2012**, *3*, 1049. (i) Guo, Z.; Nam, S.; Park, S.; Yoon, J. *Chem. Sci.* **2012**, *3*, 2760. (j) Fu, N.; Su, D.; Cort, J. R.; Chen, B.; Xiong, Y.; Qian, W.-J.; Konopka, A. E.; Bigelow, D. J.; Squier, T. C. *J. Am. Chem. Soc.* **2013**, *135*, 3567.
- (5) For selected literature, see: (a) Meister, A.; Anderson, M. E. *Annu. Rev. Biochem.* **1983**, *52*, 711. (b) Chen, X.; Tian, X.; Shin, I.; Yoon, J. *Chem. Soc. Rev.* **2011**, *40*, 4783. (c) Feng, Y.; Cheng, J.; Zhou, L.; Zhou, X.; Xiang, H. *Analyst* **2012**, *137*, 4885. (d) Hyman, L. M.; Fanz, K. J. *Coord. Chem. Rev.* **2012**, *256*, 2333.
- (6) Dalton, T. P.; Shertzer, H. G.; Puga, A. *Annu. Rev. Pharmacol. Toxicol.* **1999**, *39*, 67.
- (7) Shao, N.; Jin, J.; Wang, H.; Zheng, J.; Yang, R.; Chan, W.; Abliz, C. *J. Am. Chem. Soc.* **2010**, *132*, 725.
- (8) Guo, Y.; Yang, X.; Hakuna, L.; Barve, A.; Escobedo, J. O.; Lowry, M.; Strongin, R. M. *Sensors* **2012**, *12*, 5940.
- (9) Niu, L.-Y.; Guan, Y.-S.; Chen, Y.-Z.; Wu, L.-Z.; Tung, C.-H.; Yang, Q.-Z. *J. Am. Chem. Soc.* **2012**, *134*, 18928.
- (10) Szaciłowski, K.; Macyk, W.; Drzewiecka-Matuszek, A.; Brindell, M.; Stochel, G. *Chem. Rev.* **2005**, *105*, 2647.
- (11) (a) Maity, D.; Govindaraju, T. *Org. Biomol. Chem.* **2013**, *11*, 2098. (b) Xu, K.; Qiang, M.; Gao, W.; Su, R.; Li, N.; Gao, Y.; Xie, Y.; Kong, F.; Tang, B. *Chem. Sci.* **2013**, *4*, 1079.
- (12) (a) Yuan, L.; Lin, W.; Zheng, K.; He, L.; Huang, W. *Chem. Soc. Rev.* **2013**, *42*, 622. (b) Guo, Z.; Park, S.; Yoon, J.; Shin, I. *Chem. Soc. Rev.* **2014**, *43*, 16.
- (13) Myochin, T.; Kiyose, K.; Hanaoka, K.; Kojima, H.; Terai, T.; Nagano, T. *J. Am. Chem. Soc.* **2011**, *133*, 3401.
- (14) Kim, J.; Lim, S.-H.; Yoon, Y.; Thangadurai, T. D.; Yoon, S. *Tetrahedron Lett.* **2011**, *52*, 2645.
- (15) (a) Hilderbrand, S. A.; Lippard, S. J. *Inorg. Chem.* **2004**, *43*, 5294. (b) Guo, Z.; Zhu, W.; Shen, L.; Tian, H. *Angew. Chem., Int. Ed.* **2007**, *46*, 5549. (c) Srivastava, P.; Ali, R.; Razi, S. S.; Shahid, M.; Patnaik, S.; Misra, A. *Tetrahedron Lett.* **2013**, *54*, 3688. (d) Biswal, B.; Bag, B. *Org. Biomol. Chem.* **2013**, *11*, 4975.
- (16) Carmona, P.; Navarro, R.; Hernanz, A., Eds. *Spectroscopy of Biological Molecules: Modern Trends*; Springer: New York, 1997.
- (17) Van de Bittner, G. C.; Bertozzi, C. R.; Chang, C. J. *J. Am. Chem. Soc.* **2013**, *135*, 1783.
- (18) Saito, C.; Zwingmann, C.; Jaeschke, H. *Hepatology* **2010**, *51*, 246.
- (19) Mitchell, D. B.; Acosta, D.; Bruckner, J. V. *Toxicology* **1985**, *37*, 127.